GESEP – Gerência de Especialistas em Sistemas Elétricos de Potência

Título:

Performance comparison of IGBTS and SIC-MOSFET applied in photovoltaic inverters during reactive power injection

Autores:

R. M. Paulo, L. A. R. Rios, W. V. Ribeiro, A. F. Cupertino e H. A. Pereira

Publicado em:

2017 Brazilian Power Electronics Conference (COBEP)

Data da Publicação:

2017

Citação para a versão publicada:

R. M. Paulo, L. A. R. Rios, W. V. Ribeiro, A. F. Cupertino and H. A. Pereira, "Performance comparison of IGBTS and SIC-MOSFET applied in photovoltaic inverters during reactive power injection," 2017 Brazilian Power Electronics Conference (COBEP), Juiz de Fora, 2017, pp. 1-6.

PERFORMANCE COMPARISON OF IGBTS AND SIC-MOSFET APPLIED IN PHOTOVOLTAIC INVERTERS DURING REACTIVE POWER INJECTION

Paulo R. M. Júnior[1], Lara A. R. Rios[1], Wesley V. Ribeiro[1], Allan F. Cupertino[1, 2], Heverton A. Pereira[1].
[1]Gerência de Especialistas em Sistemas Elétricos de Potência Universidade Federal de Viçosa – UFV, Viçosa - MG, Brazil.
[2]Departamento de Eng. de Materiais Centro Federal de Educação Tecnológica de Minas Gerais, Belo Horizonte - MG, Brazil.
e-mail: paulomatiaspq@gmail.com, laara.rodarte@gmail.com, wv.ribeiro92@gmail.com, allan.cupertino@yahoo.com.br, heverton.pereira@ufv.br.

***Abstract* - The ac-grid power quality can be significantly affected by the impact of many small photovoltaic (PV) grid-connected inverters. There are many ways to improve the system stability, regarding voltage regulation. Some works in literature propose to use the multifunctional PV inverter to support reactive power to the grid. The main drawback of this solution is the increase of losses in the converter during this additional functionality. Therefore, this paper analyzes the power losses and temperature in the PV inverter semiconductors during reactive power injection. This analysis is made using four different IGBTs technologies and one SiC MOSFET. Simulations considering a 5kW three-phase PV inverter are performed with focus in the comparison between these five semiconductor devices.**

***Keywords* - Power quality, PV Inverter, SiC-MOSFET, solar energy, switching losses, thermal models.**

I. INTRODUCTION

The installation of solar photovoltaic (PV) power plants have increased considerable around the world in the last decades. The installed and commissioned power in PV systems reach 50.6 GW in 2015, showing a growth of 25.6% over the 40.3 GW commissioned in 2014. The cumulative installed solar PV power capacity increased 29% year-on-year, at the same time that the PV system prices declines of around 75% in less than 10 years [1]. However, with the progress of the renewable energy, including the photovoltaic sources, the concern about the grid power quality grows too, mainly due to the use of power electronic based-converters.

In this context, there has been growing interest in the use of multifunctional inverters [2] [3]. Thus, in addition to photovoltaic inverters perform only the task of providing active power during the day, they can also assist the main grid with reactive power support at night or during low-profile irradiance [4]. Nevertheless, this new functionality results in an extra work time which can affect the inverter efficiency and lifetime [5].

The power modules, are the most sensible components of the PV inverters in terms of thermal effects [6]. The thermal stresses affect the reliability, causing more power losses and also, are one of the most observed factors of failures in power devices [7]. From all factor aforementioned, there is an increasing demand for devices that are capable of faster switching, higher power rating, lower switching losses, and higher temperature capability [8].

In the semiconductor technology area, the development of SiC transistors has grown as these devices have better characteristics when compared to the Si semiconductors. SiC semiconductor devices are expected to have high temperature, high speed and high voltage operation capabilities, which are attributed to the wide bandgap properties of SiC [9]. Thereby, it grows the interest in the study of the SiC MOSFET (Silicon Carbide Metal Oxide Semiconductor Field Effect Transistor) to replace Si IGBT (Silicon Insulated Gate Bipolar Transistor) used in PV inverters.

This paper provides a comparative analysis of two types of semiconductors, the IGBT and the SiC MOSFET, applied in a three-phase PV inverter. The comparison is focused in the conduction and switching losses in semiconductor switches (IGBTs and MOSFETs), while reactive power injection is added as an ancillary service.

This paper is structured as follows: Section II provides the description of a three-phase grid-connected PV inverter and the control strategy implemented to regulate the active and reactive power flow. Furthermore, it is shown the data from the thermal model of the semiconductors as well as their conduction and switching losses based on datasheets in Section III. In Section IV presents the simulation and results, determining the losses of the IGBTs and the SiC MOSFET when active and reactive powers were injected in the inverter. Conclusions are state in Section V.

II. CONTROL STRATEGY

The system studied in this work is composed of a three-phase grid-connect inverter as shown in Figure 1. The inverter has a LCL filter and its dc side is connected in the solar array. Generally, in power electronics applications, currents loops are used to protect the inverter from overcurrent. The control is made in synchronous reference frame, presenting faster internal loops to control the direct and quadrature axis currents. Furthermore, the structure includes slower external loops, in order to control the dc bus voltage and the reactive power injected into the grid. Finally, a Phase Locked Loop (PLL) structure is used in order to synchronize the system. The complete control strategy is presented in Figure 2.

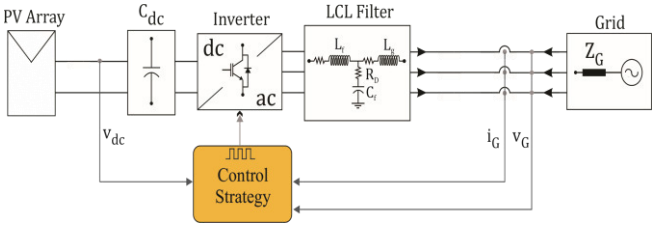

Fig. 1. Three-phase photovoltaic inverter connected to grid.

978-1-5090-6248-5/17/$31.00 ©2017 IEEE

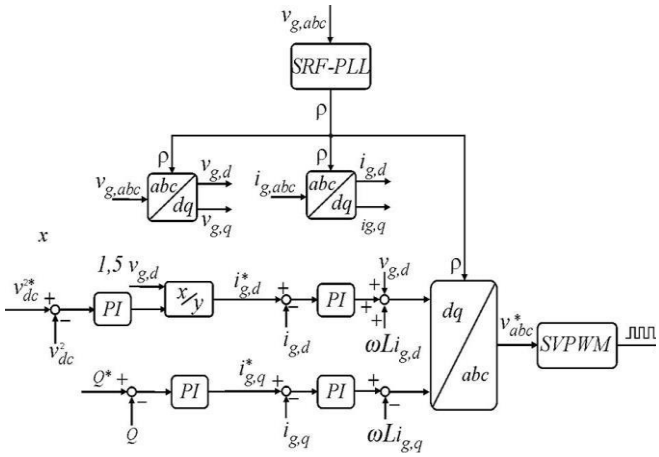

Fig. 2. Complete control structure.

A. Current Control Loop

In this control strategy, the closed-loop transfer function is given by:

$$\frac{I_{d,q}(s)}{I^*_{d,q}(s)} = \frac{k_{p,c}/L}{s + k_{p,c}/L}, \tag{1}$$

where $L = L_f + L_g$ and $L_f = L_g$, from the equivalent simplified circuit of the LCL filter.

Since the PV inverter plants for direct and quadrature current axis are equal, it can be used the same gains for both current loops. Also, the parameters of the PI controller are found using the method of poles placement. The current loop gains and the others parameters are discussed later.

B. Reactive Power Control Loop

The closed-loop transfer function of the reactive power loop is described by:

$$\frac{Q(s)}{Q^*(s)} = \frac{1 + T_1 s}{1 + T_2 s}, \tag{2}$$

where $T_2 = \frac{1+Hk_{p,\text{reac}}}{Hk_{i,\text{reac}}}$, $T_1 = \frac{k_{p,\text{reac}}}{k_{i,\text{reac}}}$, $H = -\frac{3}{2}v_g$ and v_g is the grid voltage.

Considering again the poles placement method, it is possible to define the PI controller gains.

C. DC Bus Voltage Control

The equation describing a dc bus system is given by:

$$\frac{\boldsymbol{dv_{dc}^2}}{\boldsymbol{dt}} = \frac{\boldsymbol{2(P_{PV} - P_C)}}{\boldsymbol{C_{dc}}}, \tag{3}$$

where P_C is the active power absorbed by the converter, P_{PV} is the active power generated in the photovoltaic panels, C_{dc} is the capacitance of the capacitor connected in the dc bus and v_{dc} is the dc bus voltage.

By applying the Laplace Transform to (3), and using a PI controller, the closed loop transfer function is given by:

$$\frac{\boldsymbol{V_{dc}^2}}{\boldsymbol{V_{dc}^{*2}}} = \frac{\boldsymbol{-2(sk_{p,bus} + k_{i,bus})}}{\boldsymbol{C_{dc}s^2 - 2(sk_{p,bus} + k_{i,bus})}}, \tag{4}$$

where the controller gains are obtained using the method of poles placement.

The semiconductor switches will be compared in a multifunctional three-phase photovoltaic inverter with switching frequencies of 12, 24 and 36 kHz. The gains of all controllers and the parameters of the LCL filter mentioned above depend on the switching frequency. The values of all parameters are shown in Table I.

TABLE I
Control Parameters

Parameters	12 kHz	24 kHz	36 kHz
$k_{p,c}$	1.531	1.531	1.531
$k_{i,c}$	14.432	14.432	14.432
$k_{p,pll}$	0.572	0.572	0.572
$k_{i,pll}$	50.895	50.895	50.895
$k_{p,reac}$	-0.0005	-0.0005	-0.0005
$k_{i,reac}$	-0.405	-0.81	-1.215
$k_{p,bus}$	0.226	0.452	0.678
$k_{i,bus}$	14.212	56.848	127.910
L_f	2.031e-4 H	1.016e-4 H	6.77e-5 H
C_f	1.558e-5 F	7.793e-6 F	5.196e-6 F
V_g	310.270 V	310.270 V	310.270 V
V_{dc}	700 V	700V	700V
R_d	0.400 Ω	0.400 Ω	0.400 Ω
C_{dc}	1e-3 F	1e-3 F	1e-3F

III. THERMAL MODEL AND LOSSES CALCULATION

The losses in an IGBT or MOSFET are given by static losses (conduction) P_{cond}, when the devices are in the conduction state, and by switching losses P_{sw}, when the devices are switching from the block stage to conduction state and vice-versa, that is:

$$\boldsymbol{P_t = P_{cond} + P_{sw}}. \tag{5}$$

The conductions losses can be calculated by:

$$\boldsymbol{P_{cond} = v_{ce0} \times i_{c,av} + r_c \times i^2_{\text{c,rms}}}, \tag{6}$$

where v_{ce0} is the voltage across the IGBT on state current collector-emitter, $i_{c,av}$ and $i_{c,rms}$ are the average collector current and root mean square collector current respectively and r_c is the collector-emitter on state resistance [10].

The switching losses are given by:

$$\boldsymbol{P_{sw} = (Es_{ON} + Es_{OFF}) \times fsw}, \tag{7}$$

where Es_{ON} is the lost energy to IGBT starts to conduct, Es_{OFF} is the lost energy to IGBT stops to conduct and f_{sw} is the switching frequency [11].

In this paper, five semiconductor switches are used: two third generation IGBTs I1 (FS15R12VT3) and I2 (FS25R12KT3), two fourth generation IGBTs I3 (FP15R12W1T3) and I4 (FS25R12W1T4), and a SiC

MOSFET (CCS020M12CM2). Their parameters are shown in Table II.

TABLE II
SEMICONDUCTOR SWICHERS

Parameter	I1	I2	I3	I4	M1
V_{CES}	1200V	1200V	1200V	1200V	1200V
$I_{C\ nom}$	15A	25A	15A	25A	20A
$T_{VJ\ max}$	150°	150°	175°	175°	150°
Generation	3rd	3rd	4th	4th	-

The thermal models of the IGBTs are implemented on PLECS simulator. The thermal impedances and the losses are based on their datasheets. The conduction and switching losses characteristics for IGBTs modules are shown in Figure 3 and Figure 4. Finally, the conduction and switching losses characteristics for SiC MOSFET are shown in Figure 5 and Figure 6.

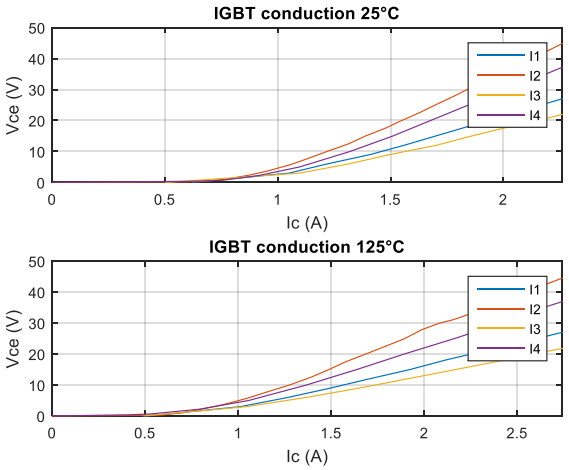

Fig. 3. IGBT's thermal models, conduction losses.

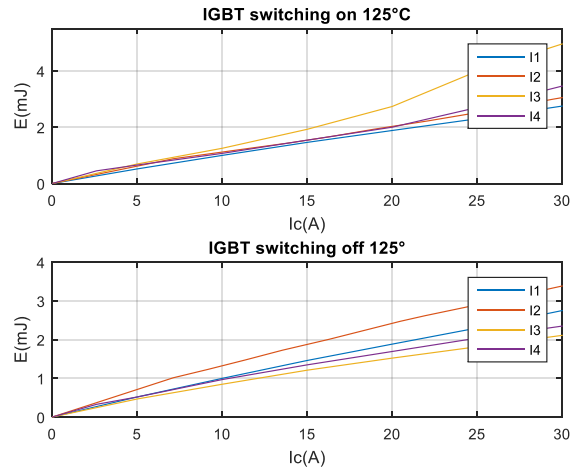

Fig. 4. IGBT's thermal models, switching losses.

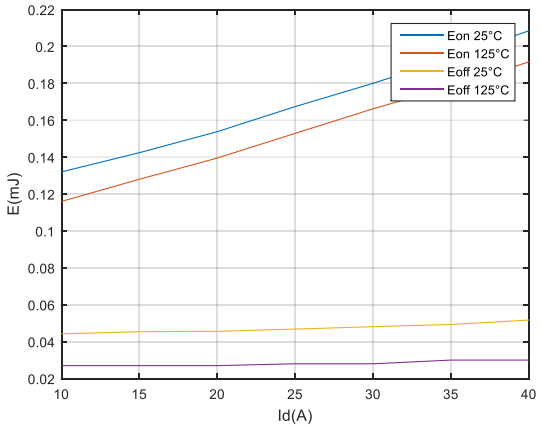

Fig. 5. SiC MOSFET thermal models, switching losses.

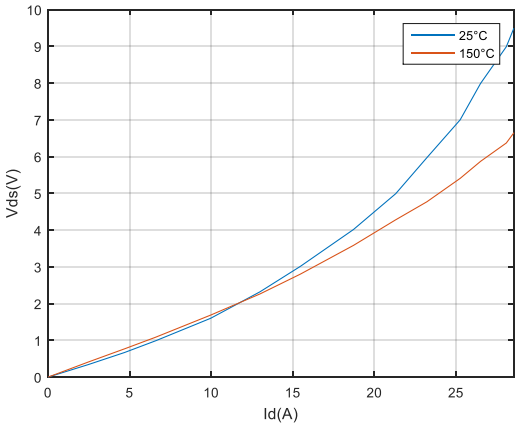

Fig. 6. SiC MOSFET thermal models, conduction losses.

IV. SIMULATION AND RESULTS

The simulation was implemented using a three-phase photovoltaic inverter connected to the grid. Switching frequencies of 12, 24 and 36 kHz are approached. The first part consists of steps in the reactive power injected in the grid of 1 to 5 kVAr, without injection of active power into the grid. In the second part, the same steps of reactive power in the grid are given as previously mentioned, and at the same time, active power steps were given in the grid, from 1 to 3 kW.

After, the power losses of all devices were evaluated. In the simulation, each device contains internally a three-phase bridge with 6 semiconductors switches and 6 diodes in antiparallel. The results for all devices, analyzing the switching losses, are illustrated in Figures 7 - 11.

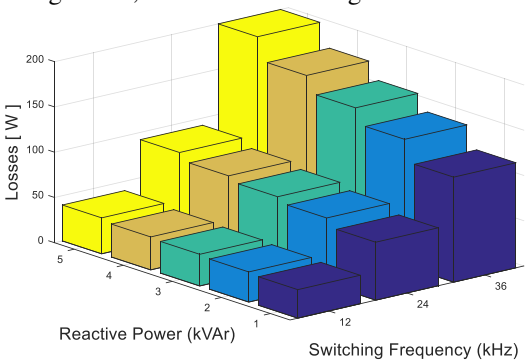

Fig. 7. Third generation IGBT 15A (I1) switching losses.

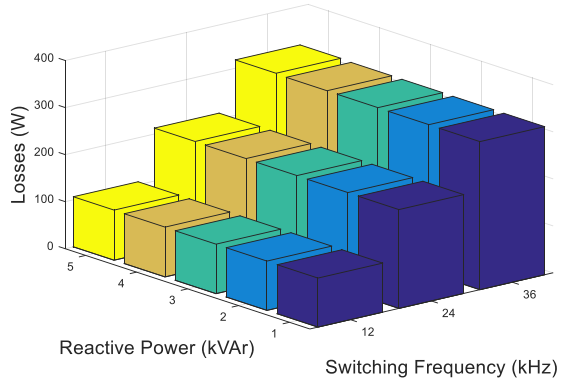

Fig. 8. Third generation IGBT 25A (I2) switching losses.

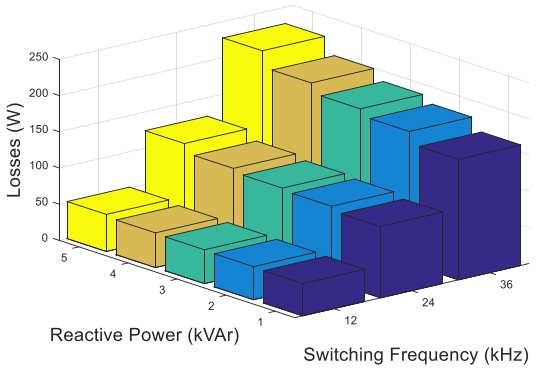

Fig. 9. Fourth generation IGBT 15A (I3) switching losses.

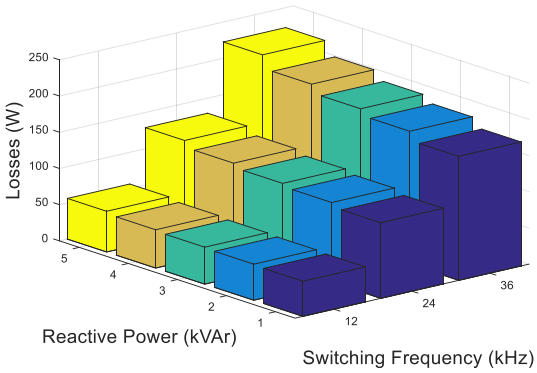

Fig. 10. Fourth generation IGBT 25A (I4) switching losses.

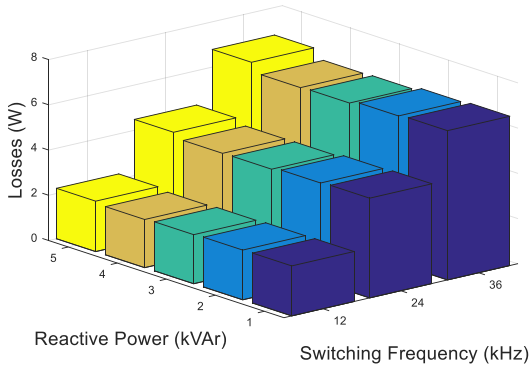

Fig. 11. SiC MOSFET (M1) switching losses.

As can be seen, the switching losses increase for higher frequencies, as expected by (7). Another interesting fact is that there is not a significant losses increasing for higher reactive power values, being the main variation due to the switching frequency. As observed, there are a large loss difference between the Si IGBTs and the SiC MOSFET. The SiC device presents less losses than the Si components, and this difference is very significant. Thus, it shows an advantage of using this new technology.

Regarding conduction losses, it is observed that there is no significant change in losses by the switching frequency change, once the conduction loss given by (6) does not depend on the switching frequency. The losses of all devices for 36 kHz switching were then measured, and the results are shown in Table III.

TABLE III
CONDUCTION LOSSES (W) – REACTIVE POWER – 36 kHz

Power (kVAr)	I1	I2	I3	I4	M1
1	10.211	8.514	11.201	9.111	4.571
2	11.315	9.321	12.404	10.010	5.141
3	13.216	10.714	14.608	11.571	6.151
4	15.818	12.616	17.803	13.751	7.612
5	19.312	15.011	22.471	16.616	9.413

In Table III, it is possible to note the smaller losses in the SiC MOSFET if compared to the other devices analyzed in this project; however, the difference is not as expressive as the switching losses. It can be conclude that the great difference between the semiconductors is due to the losses by the switching. Tables IV, V and VI show the total power losses, the sum of the switching and conduction losses, for the frequencies of 12, 24 and 36 kHz respectively.

TABLE IV
TOTAL LOSSES (W) - REACTIVE POWER - 12kHz

Power (kVAr)	I1	I2	I3	I4	M1
1	64.501	112.550	54.946	56.628	10.513
2	67.003	113.602	58.056	58.899	10.897
3	69.511	115.103	61.149	61.399	11.978
4	73.320	117.412	65.178	65.173	13.687
5	79.905	120.003	72.137	70.716	15.914

TABLE V
TOTAL LOSSES (W) - REACTIVE POWER - 24kHz

Power (kVAr)	I1	I2	I3	I4	M1
1	128.831	218.503	110.608	114.444	11.317
2	137.418	219.819	120.335	123.29	12.691
3	143.503	221.704	128.672	131.455	15.163
4	152.208	224.105	140.164	140.825	18.637
5	165.501	228.103	156.454	154.597	22.825

TABLE VI

TOTAL LOSSES (W) - REACTIVE POWER - 36kHz

Power (kVAr)	I1	I2	I3	I4	M1
1	204.902	323.204	180.555	182.868	11.424
2	224.630	324.520	205.258	201.764	12.939
3	237.612	326.511	225.649	218.732	15.545
4	252.803	328.802	252.444	239.772	19.227
5	275.401	332.807	289.452	267.882	23.455

As noticed before, the greater source of losses is the switching. Thus, analyzing the results, it can be seen that the losses increase according to the switching frequency. The greater conduction loss for each generation is on I1 and I3, respectively, since these devices present a smaller rated current than I2 and I4. Thereby, components with higher nominal values present less losses when used in the same application of lower components.

Considering the total losses, it is observed that for the third generation IGBTs, I1 presented higher losses than I2, whereas, for the fourth generation IGBTs the total losses don't have a significant difference. On the other hand, the M1 still presents less losses and less variation by the switching frequency than the other semiconductors.

In the last simulation the active and reactive power are applied together. Using the schematic thermal Foster model [12], the temperature variation on the semiconductor switchers are estimated and can be verified in Figures 12 - 16. Through the analysis of the figures, it is perceptible that the SiC MOSFET achieved a better performance with regard to the temperature. Moreover, there is not a significant difference between the devices temperature caused by injecting active power or reactive power separately.

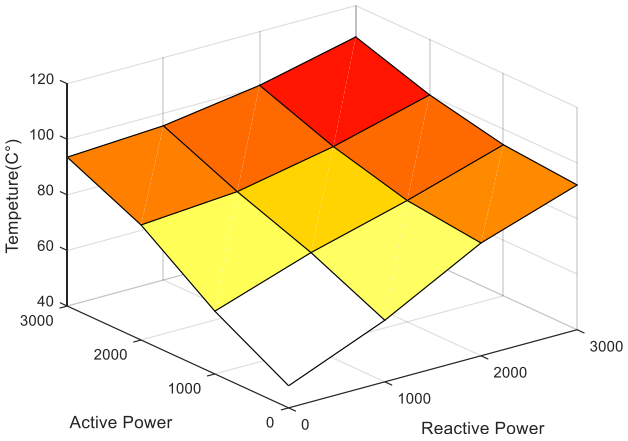

Fig. 12. Average temperature for the 3rd generation IGBT 15A (I1) for active and reactive power.

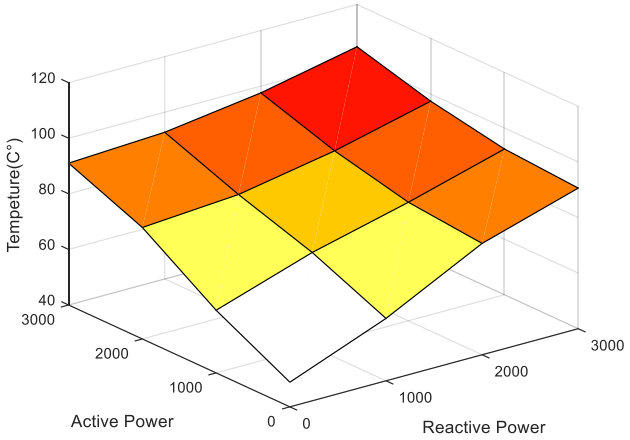

Fig. 13. Average temperature for the 3rd generation IGBT 25A (I2) for active and reactive power.

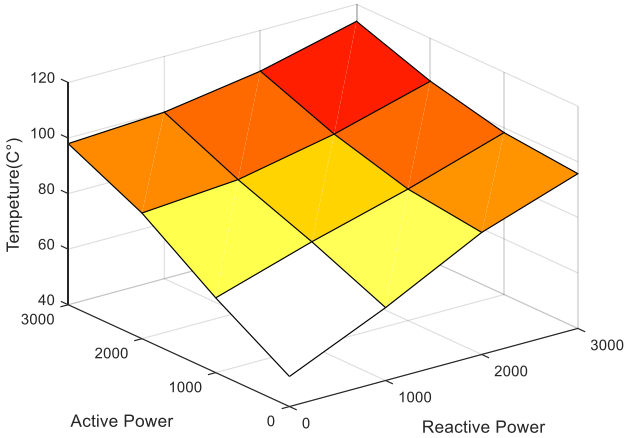

Fig. 14. Average temperature for the 4th generation IGBT 15A (I3) for active and reactive power.

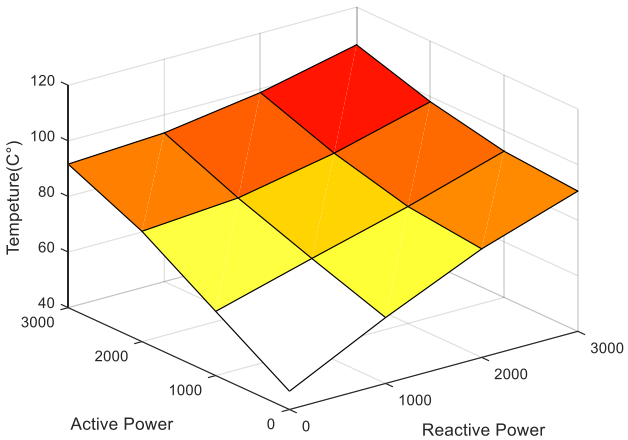

Fig. 15. Average temperature for the 4th generation IGBT 25A (I4) for active and reactive power.

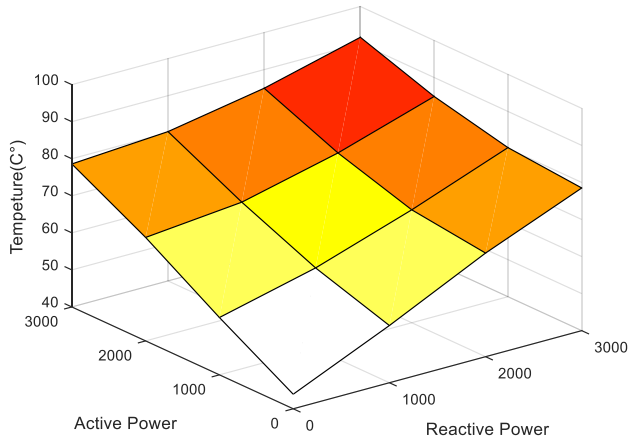

Fig. 16. Average temperature for the SiC MOSFET 20A (M1) for active and reactive power.

Based on the analysis presented, it can be concluded that the SiC MOSFET had a better performance (less losses and lower temperature) when compared to the IGBTs due to the characteristics of Silicon Carbide devices.

In addition, comparing the IGBTs can be seen the temperature difference between the semiconductors of the same generation. The 25A IGBTs reach lower maximum temperature than the 15A IGBTs.

IV. CONCLUSIONS

In this paper, four Si IGBTs and one SiC MOSFET are compared regarding their conduction and switching losses in a three-phase photovoltaic inverter connected to grid. The results show that the SiC MOSFET has much lower loss compared with the Si IGBTs availed in this paper. The SiC conductor presents a better performance both in losses and reached temperature.

Moreover, the Si IGBT switching loss increase significantly with increasing switching frequency; this fact is not observed in SiC MOSFET. In addition, it has been observed that the temperature of SiC MOSFET is much lower than the Si IGBTs temperature.

Additionally, the increase of the rated current of the device reduces the power losses and consequently the junction temperature of the devices. This fact can be verified when the 15 A and 25 A devices of same technology are compared..

In fact, the definition of the power devices employed in a photovoltaic inverter are related to other variables as reliability, costs and power density. The analysis of these parameters is out of the scope of this work and can be approached in future works.

ACKNOLEDGEMENTS

The authors would like to thank the Brazilian agencies CAPES, FAPEMIG and CNPq, which support this work.

REFERENCES

[1] EPIA, “Global Market Outlook for Solar Power / 2016 - 2020,” no. February, p. 40, 2016.

[2] R. M. Domingos, L. S. Xavier, A. F. Cupertino, and H. A. Pereira, “Current control strategy for reactive and harmonic compensation with dynamic saturation,” IEEE Int. Symp. Ind. Electron., vol. 2015–Septe, pp. 669–674, 2015.

[3] S. Ozdemir, S. Bayhan, I. Sefa, and N. Altin, “Three-phase multilevel grid interactive inverter for PV systems with reactive power support capability,” 2015 1st Work. Smart Grid Renew. Energy, SGRE 2015, 2015.

[4] R. K. Varma, B. Das, I. Axente, and T. Vanderheide, “Optimal 24-hr utilization of a PV solar system as STATCOM (PV-STATCOM) in a distribution network,” IEEE Power Energy Soc. Gen. Meet., pp. 1–8, 2011.

[5] A. Anurag, Y. Yang, and F. Blaabjerg, “Thermal Performance and Reliability Analysis of Single-Phase PV Inverters with Reactive Power Injection Outside Feed-In Operating Hours,” IEEE J. Emerg. Sel. Top. Power Electron., vol. 3, no. 4, pp. 870–880, 2015.

[6] S. M. Sreechithra, P. Jirutitijaroen, and A. K. Rathore, “Impacts of reactive power injections on thermal performances of PV inverters,” IECON Proc. (Industrial Electron. Conf., pp. 7175–7180, 2013.

[7] I. Ndiaye, X. Wu, and M. Agamy, “Impact of Micro-inverter Reactive Power Support Capability in High Penetration Residential PV Networks,” 2015.

[8] O. Sivkov and M. Novak, “Implementation of SiC inverter for high frequency, medium voltage applications,” Proc. 16th Int. Conf. Mechatronics, Mechatronika 2014, pp. 477–483, 2014.

[9] T. Funaki et al., “Power conversion with SiC devices at extremely high ambient temperatures,” IEEE Trans. Power Electron., vol. 22, no. 4, pp. 1321–1329, 2007.

[10] E. G. De Andrade, H. A. De Oliveira, V. Ribeiro, R. C. De Barros, and H. A. Pereira, “Power Losses in Photovoltaic Inverter Components due to Reactive Power Injection,” 2016.

[11] H. Tanabe, T. Kojima, A. Imakiire, K. Fuji, M. Kozako, and M. Hikita, “Comparison performance of Si-IGBT and SiC-MOSFET used for high efficiency inverter of contactless power transfer system,” Proc. Int. Conf. Power Electron. Drive Syst., vol. 2015–Augus, no. June, pp. 707–710, 2015.

[12] X. Hu, S. Lin, S. Stanton, and W. Lian, “A Foster network thermal model for HEV/EV battery modeling,” IEEE Trans. Ind. Appl., vol. 47, no. 4, pp. 1692–1699, 2011.